Imaging within Scattering Media using Two-Photon Excitation

Jeremias Püls

Master Thesis
Supervised by Dr. Edouard Berrocal
Co-supervised by Dr. Joakim Bood

Division of Combustion Physics
Lund University

VT 2016

LUND
UNIVERSITY

June 2016
Lund Reports on Combustion Physics, LRCP-197
ISNR LUTFD2/TFC-197-SE
ISSN 1102-8718

Jeremias Püls
Divison of Combustion Physics
Department of Physics
Faculty of Physics
Faculty of Engineering LTH
Lund University
P-O Box 118
S-22100 Lund
Sweden

Abstract

Imaging in scattering media is used in different fields such as medicine for the diagnosis of tissues or in combustion to study spray injection systems. The problem with imaging in scattering media is the blurring induced by multiply scattered photons. There exists techniques to reduce multiple scattering detection, based on various filtering approaches.

Two-photon excitation fluorescence imaging, which is the approach proposed in this thesis, fundamentally varies from the other, existing concepts: Instead of filtering the light before detecting it, two-photon excitation fluorescence induces less multiple scattering outside the focal point of interest as scattered photons do not carry enough energy to induce fluorescence.

In this master project a suitable fluorescence dye, Fluorescein, was chosen to compare one-photon and two-photon excitation fluorescence imaging in a cuvette. The dependence of the signal on the focusing length and dye concentration was tested. The maximum signal of one-photon excitation fluorescence was independent of the focusing lens and was located at entrance of the cuvette; whereas the maximum signal of two-photon excitation was at the focal point.

Finally, the intensity and the image contrast were measured with and without particles. A contrast improvement was observed with two-photon excitation fluorescence in comparison with one-photon when no scattering particles were added. Nonetheless, the contrast of 1PE was higher than the contrast of 2PE fluorescence after the scattering particles were added into the cuvette.

Since the signal depends quadratically on the laser intensity, a laser with a higher pulse power is believed to improve the contrast significantly. As a conclusion, such a laser system is needed in order to further test two-photon excitation fluorescence imaging in turbid media.

Acknowledgements

First of all I want to thank my main supervisor Edouard for his guidance and mentorship during the project. I like his approach of having fun and working hard. Additionally, I want to thank Joakim Bood not only for his theoretical support but also for evoking my interest for this field during the LiDAR project, which was part of the "Atomic and Molecular Spectrocopy" course. Thanks to Igor for restoring files from the broken university laptop. Thanks to my friends at the university, Sukant, Johan, Tasnimul, Benjamin and Said, for the moral support as well as the fun time we had together and their input and ideas about my project. The software Inkscape was used for the drawings in my thesis report and I would like to acknowledge Alexander Franzen for developing the component library.

I also want to thank my parents for their support. Last but certainly not least a stort tack to my girlfriend Elin for her constant encouragement during the thesis life ♡.

Contents

Acronyms

1PE	one-photon excitation
2PE	two-photon excitation
cw laser	continuous-wave laser
OKE	optical Kerr effect
SLIPI	Structured Laser Illumination Planar Imaging
SNR	signal-to-noise ratio

Chapter 1

Introduction

1.1 Motivation

Using laser imaging techniques, it is possible to perform in vivo diagnosis in turbid media such as blood or skin without any harm [1], [2]. Light scatters multiple times in such media, thereby blurring the final image, and making it difficult to image within them.

Another application of laser diagnostics in turbid media is spray imaging. By increasing visibility of the liquid injection, it is possible to further optimize the combustion process [3]. In times of climate change, pollution and fluctuating oil price, improving combustion processes is not only interesting from a scientific point of view, but also for society.

When light scatters multiple times it loses its initial optical properties, such as coherence, pulse duration, direction etc. There exist different optical filtering techniques that take advantage of the alteration of the light and can suppress the multiply scattered light. Fourier filtering is based on the geometric properties of the light, where an aperture is placed around the focal point of the lens. Non-collinear (multiply scattered) light is not focused and blocked by the aperture. Another approach is to place two linear polarizaton filter at both sides of the scattering medium, which is called polarization filtering [4].

Time gating is a technique were an ultra-short laser pulse is used. An ultra fast time gate in front of the detector transmits only the non-scattered light is detected [5].

Instead of placing the detector at the other side of the turbid medium, called transmission imaging, it is possible to form a laser sheet and place the camera on the side of the scattering medium. If the optical depth increases, blurring effects from multiple scattering will appear on the image. An approach to reduce those effects is to combine structured illumination with planar imaging. This technique, known as Structured Laser Illumination Planar Imaging (SLIPI), was developed by Berrocal et al [6]. However, SLIPI needs three sub-pictures to build one final image at full resolution. Fewer pictures will decrease the image resolution. Another image artifact is the absorption of laser light following the Beer-Lambert law.

The concept proposed in this thesis is fundamentally different from the existing approaches. Instead of filtering the multiply scattered light, two-photon excita-

tion (2PE) fluorescence induces by its excitation process significantly less multiple scattering. 2PE excites the fluorescence dye with twice the wavelength to induce fluorescence. For this non-linear process to happen a high photon-flux density is needed, which requires a powerful laser. A single scattered photon of the excitation source does not carry enough energy to excite the dye.

Although the concept of two-photon excitation is well known in life science microscopy, there exists less literature on two-photon excitation applied to turbid media. This thesis focuses on:

- Identifying a dye that fulfills the following criteria: non toxic, not solid, soluble in water and with a quantum yield for 2PE as high as possible in the wavelength range of $750 - 800\,\mathrm{nm}$
- Planning and building an experimental setup, where the 2PE fluorescence can be studied and compared to the one-photon excitation (1PE) fluorescence signal, while imaging a small laser light sheet crossing a cuvette containing an aqueous dye solution
- Measuring and comparing the spectral response of the selected dye for 1PE and 2PE
- Analyzing the dependence of the signal for 1PE and 2PE fluorescence in respect to the focal length and dye concentration
- Quantifying the performance of 2PE, when scattering polystyren are mixed in a water solution to induce multiple scattering

1.2 Two-Photon Excitation Fluorescence Process

Two-photon absorption or excitation is a nonlinear process that was theoretically derived by Maria Göppert-Mayer in 1931 and later experimentally proven after the invention of the laser [7]. Electrons within an atom can be excited from the ground state to an excited state by incoming photons, on the condition that the energy of the photon matches the difference in energy between the two states. If the electron is excited by two photons instead of one, where their combined energy satisfies the energy requirement, the event is called two-photon excitation, as shown in figure 1.1.

The excitation is not limited to only one or two photons, in principle any number of photons can be absorbed. Excitation involving two or more photons are named multiple-photon excitation.

The fluorescence signal of 1PE depends linearly on the excitation intensity. The absorption of light is described by the Beer-Lambert law

$$I(z) = I_0 e^{-\sigma N z} \tag{1.1}$$

where $I(z)$ is the intensity of the laser beam in respect to distance, σ_{a1} the one-photon absorption cross-section, N the concentration (number of particles per m^3) and z the traveled distance within the absorbing media.

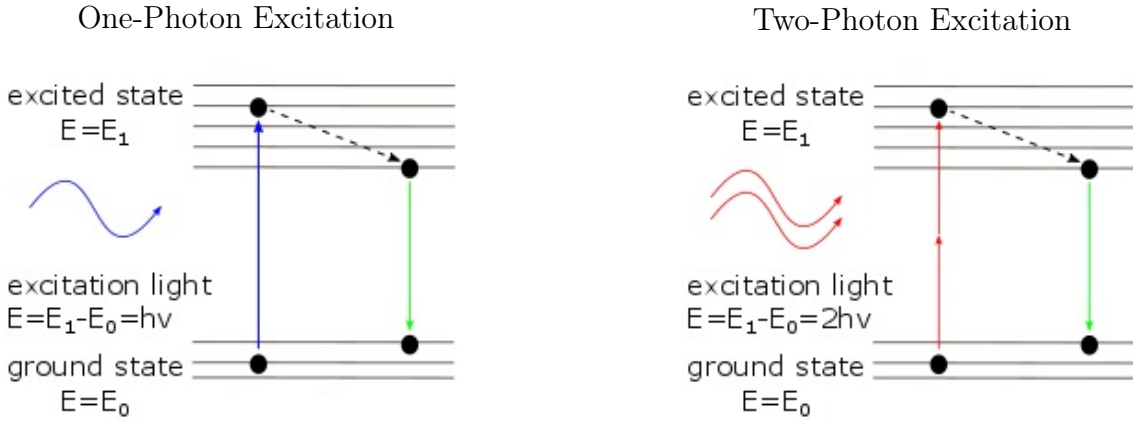

Figure 1.1: One- and two-photon excitation fluorescence in a Jablonski diagram.

The fluorescence signal of 2PE depends quadratically on the excitation intensity. The absorption of light is described as:

$$I(z) = \frac{I_0}{1 + N\sigma_2 z I_0} \tag{1.2}$$

where σ_{a2} is the absorption cross-section in GM $= 10^{-50} \frac{\mathrm{cm}^4\mathrm{s}}{\text{photons molecule}}$ named after Göppert-Mayer. GM is an unusual unit for a cross-section, because it is adapted to match the modified Beer Lambert's law equation, see Eq. 1.2. The relation of the absorption emphasizes why this technique would be of great use for imaging in turbid media. While for 1PE the fluorescence signal extinguishes exponentially according to Beer-Lambert law, it drops proportional to $\left(\frac{1}{1+z}\right)$ for two-photon excitation.
The absorption cross-section for the dye used in the experiment is shown in figure 3.2. Dyes commonly used for 1PE have a two-photon absorption cross-section of about 10 GM. Xu et al. have experimentally shown that it is possible to create materials with a cross section of 1000 GM [8].

Selection rules govern the allowed transition within an atom. The transition rules are different for one- and two-photon excitation. Due to the orbital momentum conservation, excitation from 1S to 2S is forbidden for single photon absorption, but it is allowed for two photon excitation.

The excitation spectrum for one- and two-photon excitation is not solely different by a factor of two.

The virtual or intermediate state between ground and excited state has a small lifetime, therefore a high photon flux density is required to induce two-photon absorption, which is usually sustained by a focused pulsed laser. Since two-photon absorption depends quadratically on the intensity, it can surpass one-photon absorption at high energy. It has, thus, has a wide range of applications, such as microfabrication, three-dimensional data-storage and microscopy [9].

Chapter 2

Strategies for Imaging in Scattering Media

One can either probe the scattering medium itself or a target clouded by the surrounding scattering particles. In both cases light randomly interacts multiple times with the randomly distributed scattering particles. The photons thereby lose their initial optical properties, such as direction, polarization, coherence and pulse duration. In imaging, these multiple scattering interactions, results in blurring effects on the image. There are different imaging approaches, depending on the position of the laser source in respect to the camera:

- Transillumination detection: the camera is placed behind the scattering medium to capture the light that passes through (line-of-sight configuration). This technique aims to only capture the unscattered (ballistic) photons and block the singly- or multiply scattered photons
- Side-scattering detection: the camera is placed on the side of the scattering medium, usually positioned at 90° to the incident light direction. This technique aims to only capture the singly scattered photons and block the multiply scattered photons
- Back-scattering detection: the camera is placed on the same side as the light source. This technique aims to only capture the singly scattered photons and block the multiply scattered photons

There are different filtering strategies, to remove multiple scattered light. Most of them work for transillumination imaging.

2.1 Polarization Filtering

Polarization filtering is an inexpensive and easy to implement transillumination technique to reduce the noise from multiple scattering using the polarization properties of the incident light. Photons that are multiply scattered within the sample lose their polarization and consist of an equal part of parallel and perpendicular polarization, while ballistic components keep their original polarization state. Demos et al. [4] have shown that at times longer than the arrival of the ballistic photons the original polarization is still dominant until 100 ps. At this point the polarization is equally distributed between parallel and perpendicular polarization.

As illustrated in figure 2.1, the incoming laser light is polarized linearly by a polarization filter before entering the turbid medium. Another polarizer is placed in front of the camera, oriented the same direction as the first polarizer. Since the polarization of the ballistic photons did not change the ballistic photons pass, while half of the multiply scattered photons are cut.

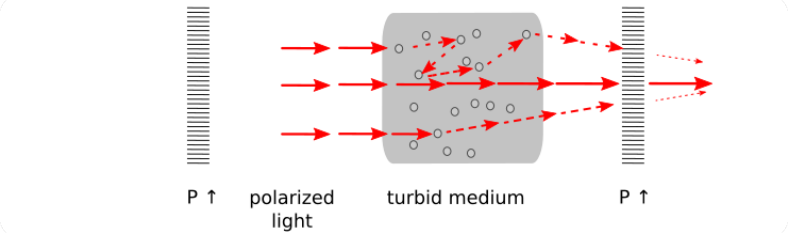

Figure 2.1: Figure 2.1 illustrates a schematic setup of polarization filtering in order to block the multiply scattered light. The continuous arrows represent the unscattered (polarized) light, while the dashed arrows represent scattered photons. The linear polarizers (P1 and P2) are oriented in the same direction. The smaller width indicates that part of the scattered light is cut by the polarization filter.

2.2 Fourier Filtering

Fourier filtering takes advantages of another light characteristic, its direction, which is altered when the light scatters. Consequently the aligned ballistic light remains parallel, while the singly or multiply scattered light does not.

A lens is placed after the turbid medium, to take advantages of the different geometrical behavior between ballistic and singly or multiply scattered light. The collimated (unscattered) light is focused at the focal point, while the singly or multiply scattered light is not focused. By using an aperture placed in the Fourier plane of the collecting lens, light scattered off axis can be suppressed. An array pattern, such as a CCD or CMOS is placed at the image plane in order to capture the image. A schematic sketch of Fourier filtering is shown in figure 2.2

2.3 Time Gating

Time gating is another approach to reduce the blurring effects from multiple scattering. It is a more complex and costly concept than Fourier and polarization filtering. As shown in figure 2.3, the ballistic photons reach the detector before the multiply scattered photons. The aim of the approach is to take advantage of this characteristic by gating the light reaching the camera in order to only capture the signal during the arrival time of the ballistic photons. Mechanical shutters are too slow, therefore a ultra fast optical gate such as the OKE (Optical Kerr Effect) gate, consisting of a Kerr medium and two polarization filter, is used. Time gating can be used for transillumination or back-scattering detection [10].

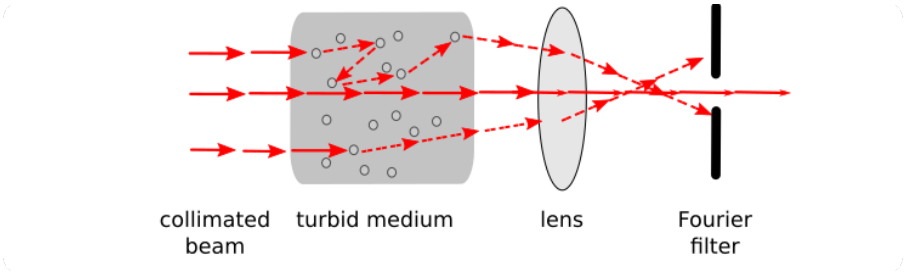

Figure 2.2: A schematic setup of Fourier filtering in order to block the multiple scattering. The dashed lines represent the multiply scattered light, while the continuous lines represent the ballistic photons.

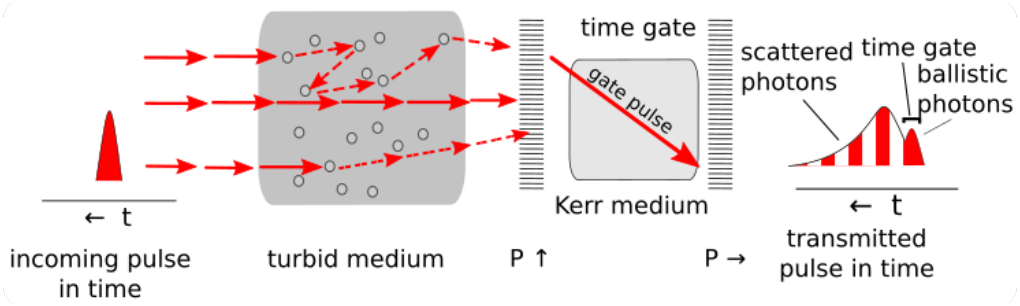

Figure 2.3: Schematic illustrating time gating. Located on the left of the scattering medium is the incoming pulse and on the right the outgoing pulse. The single and multiply scattered laser photons spread in time, while the ballistic photons exit the medium first.

The pulse from the femto second laser is splitted by a beam splitter. One part of the pulse travels to the gate and the other one interacts with the sample, the detector pulse. The OKE gate operates in a similar way as a transistor, where in this analogy the base current is represented by the gate pulse. When the gate current is applied the transistor is "on" and current passes through, vice versa when no gate current is applied. The same is true for the OKE gate. When no gate pulse is present, the device blocks the light and vice versa when gate pulse is present.

The amount of light that is transmitted through depends on the intensity of the laser pulse as well as the Kerr-constant. When an electric field (in this case the laser pulse) is present the CS_2, a commonly used Kerr medium, changes the refractive index along one axis according to

$$\Delta n = \lambda K |E|^2 \tag{2.1}$$

where K is the Kerr constant, E the strength of the electric field and λ the wavelength. When no pulse is present it acts like a glass cell.

The time window is determined either by the duration of the pulse or the relaxation time of the Kerr medium, whichever is longer. Since the pulse is in the femto scale and CS_2 has a molecular relaxation time of $\sim 2\,\text{ps}$, the relaxation time

is usually the decisive parameter [11].

When the gate pulse and the detector pulse are non-collinear, so that the gate pulse arrives at the Kerr medium with an angle the induced birefringent is not the same over the whole medium. Thus the transmission of the OKE gate is not uniform, which in turn effects the image quality, because the transmittance is not uniform over the whole OKE gate. H. Purwar et al. [5] have shown a setup where they use collinear pulses with different wavelength for gate and detector pulse to improve the image quality. A dichroic mirror is used to filter out the gate pulse after the Kerr medium.

2.4 Structured Illumination

Structured illumination was firstly introduced by Neil et al [12] to better implement optical sectioning. In addition to improve the spatial resolution and producing high contrast images, a structured illumination microscope rejects the out of focus photons, because the projected modulation disappear rapidly with the out-of-focus distance [13] provided the high enough frequency of the grating.

Structured illumination can also be used to increase image contrast in scattering environments and is flexible in a way that it does not only work in a transillumination approach, but also for side- and backscattering detection. A transillumination setup is assumed in figure 2.4. The basic idea is to modulate light intensity sinusoidally by placing a grating in the beam path before it enters the turbid medium. When photons are scattered, they lose the modulation information, while ballistic photons keep the modulation information, see figure 2.4. The illumination provides an image with intensity matrix I(x,y)

$$I(x, y) = I_C + I_S.cos(2\pi vy + \theta_0)$$

where I_C is the unmodulated light from the multiply scattered photons and I_S is the modulated light, which consists of the ballistic photons in a transmission detection and the singly scattered photons for side and back scattering detection. Three images are taken with a phase shift of $\Delta\theta = \frac{2\pi}{3}$ in between them to construct the I_S image by applying Eq. 2.2 .

$$I_S = \frac{\sqrt{2}}{3} \cdot \sqrt{(I_{\frac{2\pi}{3}} - I_0)^2 + (I_{\frac{2\pi}{3}} - I_{\frac{4\pi}{3}})^2 + (I_{\frac{4\pi}{3}} - I_0)^2} \tag{2.2}$$

If the optical depth increases, photons will be more scattered, reducing the intensity of I_S until there is no modulation left. This reduction in modulaton depth is related to the Beer-Lambert law for 1PE.

A technique based on structured illumination is Structured Laser Illumination Planar Imaging (SLIPI). It was introduced by E. Berrocal et al. [6] to experimentally approach the multiple scattering issue for planar imaging. As SLIPI is a planar

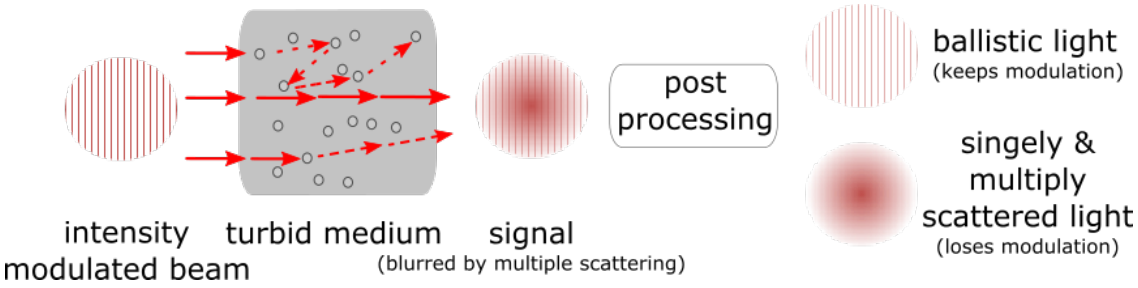

Figure 2.4: A schematic sketch illustrating structured illumination. The intensity modulated beam loses its structure after scattering. Through post-processing the induced blurring effect of scattering can be removed.

image technique it is not line-of-sight limited. Even though it is possible to get rid of multiply scattered photons in the final image, they are still captured. A laser technique that would decrease the "multiple scattering noise", before the signal arrives at the detector, would allow to increase the noise ratio and the image contrast.

2.5 Advantages of Two-Photon Fluorescence Imaging

To improve planar imaging one would need to work on three main issues for planar imaging [6], namely

- the extinction of the light according to Beer-Lambert law
- the attenuation of the signal between the laser sheet and the camera
- the unwanted signal from multiple scattering.

The approach of 2PE fluorescence is the same as for 1PE, but the laser source is replaced by a femto second producing twice as long wavelength. The incoming light excites the fluorescent dye which marks the object of interest, within the scattering medium.

Figure 2.5 graphically describes the interaction of the incoming photons for 1PE (blue light) and 2PE (red light). Let us study in more detail which interactions happen in both cases. For the blue light, a single photon carries enough energy to induce fluorescence everywhere in the turbid medium. The light induces fluorescence when it enters the medium. The fluorescence signal can be reabsorbed or scattered on the way to the detector, thus inducing a blurring effect on the final image. Furthermore the light can also scatter before it induces fluorescence and then induce fluorescence at a point outside the imaged plane. This out of focus signal can reach the detector and thereby increase the noise level on the final picture.

2PE also has to deal with the difficulty that the fluorescence signal is scattered or reabsorbed on the way to the detector. One of the advantages is that a single photon does not carry enough energy to induce fluorescence. Consequently, noise due to scattering from red photons is unlikely to generate a signal outside the

focal plane. Since 2PE fluorescence depends quadratically on the intensity of the light, it is additionally controllable via the focusing lens. To encounter laser light extension, one could in principle place a focal length that balances the extinction from extinction events, so that the induced fluorescence signal is more constant along the imaged plane.

To summarize, 2PE fluorescence can improve two of the three main issues for planar imaging, namely the laser light extinction and the effects from multiple scattering.

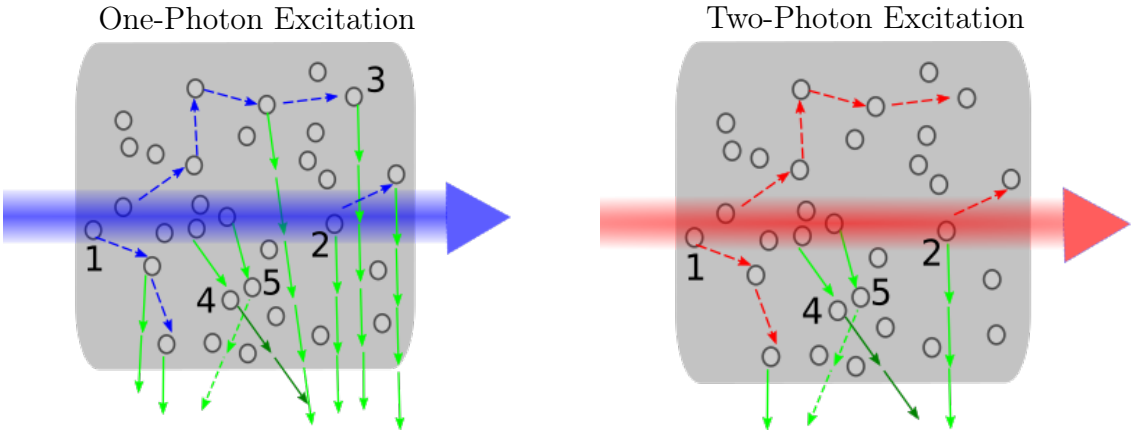

(a) (b)

1. Scattering of the excitation light
2. Excitation within the focal plane
3. Excitation outside the focal plane
4. Reabsorption
5. Scattering of the fluorescence light

Figure 2.5: The illustration depicts the different interactions for one- (figure 2.5a) and two-photon excitation (figure 2.5a) within a turbid medium. Reabsorption and scattering from the beam to the camera can happen in both cases. The multiple scattering from the red light will not induce fluorescence outside of the focal plane, while this will occur for the blue light.

Furthermore, depending on the size of the scattering particles, 2PE could improve the imaging even more. Given that the diameter of the particles is small in comparison to the wavelength of the light one can assume Rayleigh scattering. Rayleigh scattering is proportional to $\frac{1}{\lambda^4}$, so in that case a longer wavelength would drastically reduce the scattering. As the wavelength of two-photon excitation is twice as high, the scattering would reduce by a factor of 16.

Chapter 3

Experiment and Methodology

3.1 Optical Setup

A sketch of the experimental setup is shown in figure 3.1. The optical arrangement was mounted on an optical table in E234 in Enoch Thulin laboratory. Two different laser sources, a diode laser $\lambda = 447\,\text{nm}$ and a Ti:sapphire laser (Tsunami from SpectroPhysics), tunable around 800 nm were used.

Since the two-photon process demands high energy, a pulsed laser with a femto second pulse duration was used. The Ti:sapphire laser can either run in continuous or pulsed mode. The extended laser cavity features two prisms, which disperse the light. A beam cutter located between the prism, tunes the wavelength of the laser. To run in pulsed mode $\tau \sim 100\,\text{fs}$, one has to mode-lock the laser, which is done by adjusting the beam cutter. When the Ti:sapphire laser runs in continuous mode, the power is not high enough to induce two-photon excitation fluorescence according to the measurement tools used in the setup. See table 3.1 for specification about the Tsunami laser. The Ti:sapphire laser is pumped by an Nd:YLF operating at $\lambda = 532\,\text{nm}$.

Considering that the fluorescence signal for 1PE can be generated at low power, the laser source does not require to be powerful nor operate at the maximum excitation wavelength, therefore a non expensive diode laser ($\lambda = 447\,\text{nm}$) was chosen. One disadvantage of the used diode laser was that the beam has a highly diverging profile. The diode laser had a given power, to modulate the intensity a wheel filled with different absorbing neutral density filters was placed into the laser beam.

Three devices were used to detect and analyze the light namely a power-meter, to measure the power of the laser beam, a spectrometer used to modelock the Ti:sapphire laser as well as to monitor the fluorescence signal for one- and two-photon excitation and a scientific complementary metal–oxide–semiconductor (sCMOS) camera from Andor (Zyla 5.5). The camera and the cuvette containing the dye were mounted on a stage so that the distance between them could be controlled. Extension rings with a total length of 90 mm were fixed in front of the objective to magnify the area of interest, resulting in a field of view of $50 \times 140\,\text{mm}$. The focal length of the objective was 135 mm. The f-number was $f_{\#} = 4$ [1]. Two mirrors

[1] The ratio of the focal length of the lens to the diameter of the aperture. The depth of field

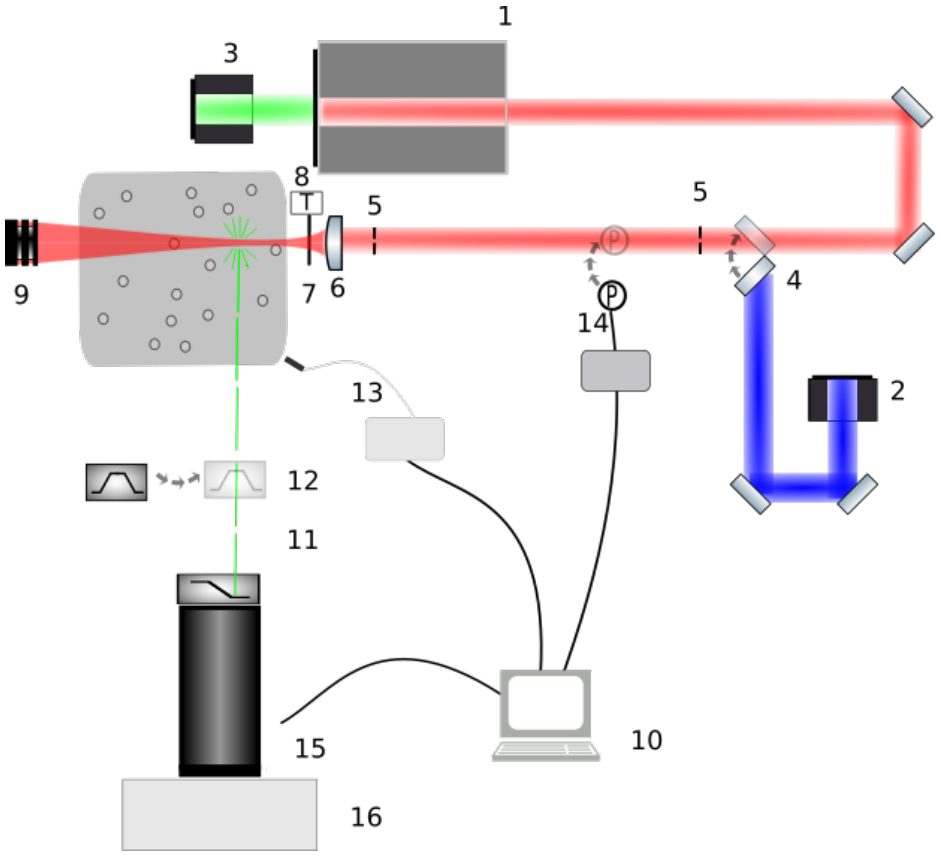

1. Ti:sapphire Laser $\lambda \sim 800\,\text{nm}$
2. CW Diode Laser $\lambda = 447\,\text{nm}$
3. CW Pump laser, Nd:YLF $\lambda = 532\,\text{nm}$
4. Flipmirror
5. Aperture
6. Cylindrical lens (50, 75, 100, 150 in mm)
7. Ronchi grating (5 lp/mm)
8. Motorized translation stage
9. Beamdump
10. Laptop
11. Short-pass filter $\lambda_{cutoff} = 750\,\text{nm}$
12. Band-pass filter $\lambda = 510 \pm 82\,\text{nm}$
13. Spectrometer
14. Powermeter
15. Objective $f = 135\,\text{mm}$
16. Zyla 5.5 from Andor, S-CMOS 2560 x 2160 pixels

Figure 3.1: A schematic of the optical setup

guided the red laser beam to the cuvette. A flipmirror was positioned to guide the the red laser along the same optical path than the red laser. The two lasers were aligned via two apertures. The laser-lightsheet was formed by placing a cylindrical plano-convex lenses in the beam path in front of the probed glass cuvette. Different cylindrical lenses with focal length of 50 mm, 75 nm, 100 nm and 150 nm were

increases in respect to the f-number

	cw mode	pulsed mode
Averaged power	0.7 W	0.7 W
Beam diameter	2 mm	2 mm
Energy per pulse		8.75 nJ/pulse
P_{Peak}		0.1 MW
Repetition rate		80 MHZ

Table 3.1: The characteristics of the Tsunami Ti:sapphire from SpectroPhysics run in continuous or pulsed mode

tested. The used lenses have a boardband dielectrc anti-reflection coating for the wavelength range of $750-1100$ nm. The used mirrors had also a coating to optimize the power of the Ti:sapphire laser. In general, most of the experiment was planned in a way to maximize the power of the Ti:sapphire laser, because the fluorescence signal of the 2PA requires high power. Whereas the 1PE the generated signal was high even at low power of the cw laser.

A low pass filter, with cut a off frequency of 750 nm, was mounted before the objective to cut of the signal from the Ti:sapphire laser. A bandpass filter (510 ± 82 nm) was mounted on a side translation stage so that it could be placed in front of the camera when the blue laser is used. The bandpass filter blocks both laser wavelengths and one third of the fluorescence signal. Since the 1PE signal was high, this reduction could be accepted. In the final experiment a Ronchi grating, $5\frac{lp}{mm}$ was added. It was mounted on a motorized translation stage to spatially modulate the light before it enters the cuvette.

Furthermore, to comply the safety standard of combustion physics, a risk evaluation was created that list all possible dangers and addresses risk reducing/controlling measures. Including the calculation of the laser safety eyewere that matches the ln-standard according to the EN207:2009.

3.2 Choice of the dye: Fluorescein

The fluorescent dye had to meet the following criteria:

- non-toxic
- soluble in water
- quantum yield for 2PE as high as possible in the range of 750 to 800 nm

The dye has to be soluble in water since the experiment is conducted in water in a cuvette. The citerion of non-toxic was set because this method may be further tested in a spray, which is not encapsulated. Fluorescein was chosen because it offers a high quantum yield for 1PE as well as for 2PE, it is non-toxic and is soluble in water. The fluorescein excitation spectrum for one-photon excitation and two-photon excitation is shown in figure 3.2.

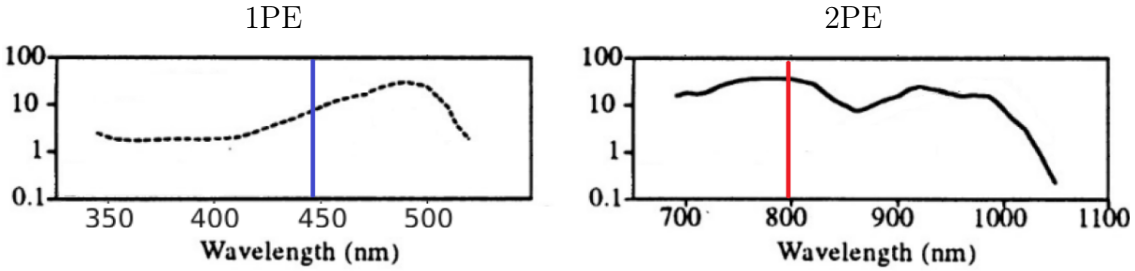

Figure 3.2: The excitation spectrum for one-photon (left) and two-photon (right) of fluorescein from [8]. The laser diode (LD) operates at $\lambda = 447\,\text{nm}$ and the tsunami at $\lambda \sim 800\,\text{nm}$. The y-axis represents the 2PE cross section in GM and the 1PE is in arbitrary scale.

3.3 Effects of Dye Concentration and Beam Focusing

The purpose of the first experiment was to investigate the influence of concentration and focusing lens on the fluorescence signal. Therefore pictures were taken with different plano-convex cylindrical lenses (50, 75, 100, 150 mm) and dye concentration. The exposure time was set to 0.1 ,0.03 and 0.001 s (1PE) respectively 1, 1 and 0.25 s (2PE) for concentration 0.0007%, 0.0021% and 0.0063%. The accumulation number was 20. For 2PE 2×2 image binning was applied. From the resulting data, a focusing lens and a dye concentration was chosen, which is suitable for the investigation in a controlled scattering medium.

Furthermore, a script was created to analyze the intensity in respect to the traveled distance inside the cuvette. The script took the average value of every column of the image matrix and normalized it by its maximum intensity.

3.4 Effects of Particles

The second test aims to compare the image quality, the intensity along the cuvette and the image contrast in scattering media between 1PE and 2PE fluorescence. Images of 1PE and 2PE fluorescence were taken at different optical depths. The exposure time was set to 0.07 s for 1PE and 1 s for 2PE . No binning was used. The optical depth was controlled by injecting particles into the aqueous dye solution. Additional to the optical depth, the position of the cuvette in respect to the laser sheet was changed, so that the fluorescence signal from the laser sheet had to travel 1, 2 or 3 cm through the cuvette. Those different distances are labeled as position 1, 2 and 3. In order to keep the same field of view, the camera was also moved to focus the new position of the signal. Therefore camera and cuvette were mounted on a translation stage. Figure 3.3 schematically indicates the different positions of the camera.

A Ronchi grating with $5\,\frac{\text{lp}}{\text{mm}}$ was mounted in front of the laser beam to modulate the light spatially. To clearly resolve the line structure of the fluorescence light, another extension ring to a total length of 100 mm was added to the camera, which resulted in a field of view of $20 \times 16\,\text{mm}$.

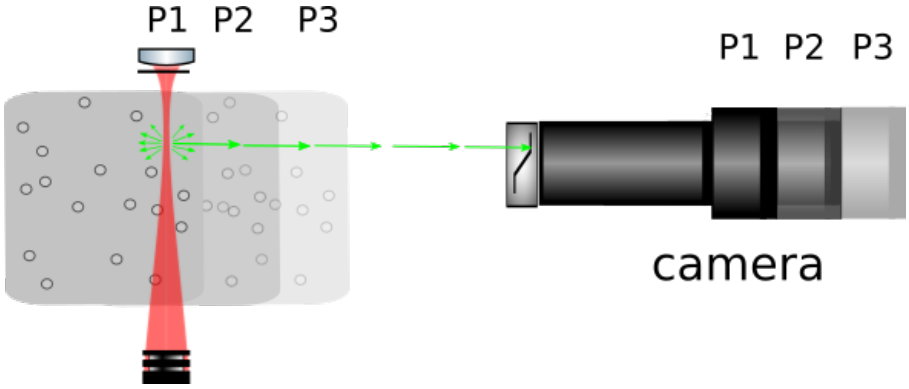

Figure 3.3: The three different camera and cuvette positions. The camera and cuvette were moved to keep the same field of view for all the three positions., while keeping focus on the light sheet.

The contrast is defined as

$$M_f = \frac{I_{\max} - I_{\min}}{I_{\max} + I_{\min}} = \frac{I_\Delta}{I_C} \tag{3.1}$$

where I_{max} and I_{min} correspond to the highest and lowest intensities, I_Δ is the amplitude of the modulation and I_C represents the mean intensity.

In the case of an sinusoidal grating of given modulation frequency f_f, the signal equals

$$I(x) = I_C + I_\Delta(sin(2\pi f_f x))$$

which complex Fourier transform has the following form

$$G(f) = a_0\delta(f) + a_f\delta(f - f_f) + a_{-f}\delta(f + f_f)$$

with $|a_f| = |a_{-f}| = \frac{I_\Delta}{2}$ and $a_0 = I_C$ results in a new form of the contrast

$$M_f = |\frac{2a_f}{a_0}|$$

For a perfect square grating (ronchi grating) the modulation in Fourier spectrum is

$$G(f) = \frac{a_0}{2}\delta(f) + \frac{a_{-f}}{\pi}\delta(f - f_f) + \frac{a_f}{\pi}\delta(f + f_f) + \text{higher frequencies}$$

Equating coefficients results in

$$M_f = |\frac{\pi a_f}{2a_0}| \tag{3.2}$$

where a_f is the fundamental component and a_0 the amplitude at zero frequency. This approach was prefered in this thesis and a Matlab script was written. The script Fourier transforms the image per column and extract a_f and a_0. Eq. 3.2 is applied to calculate the contrast.

Polystyren spheres from Bangs Laboratories were mixed into the aqueous solution to induce multiple scattering. In order to make a fair comparison, particles with

the same extinction cross section for both wavelength were mixed into the aqueous dye solution. Therefore the Rayleigh scattering regime, which has a $1/\lambda^4$ dependence [14], should be avoided. A Mie code, created by J. Jönsson and E. Berrocal, was used to test which particle diameter provides approximately the same extinction cross section for both wavelengths and how many particles are needed to create an optical depth[2] of 5. Particles with a mean diameter of $4.94\,\mu$m have an extinction cross section of approximately $5.1 \cdot 10^{-5}\,\mathrm{mm}^2$ for both wavelengths.

The density of the microspheres per ml N_ρ is $1.501{\cdot}10^9$, the length l of the cuvette is 45 mm, the by the Mie code proposed total particle number is $N_{total} = 14739$ and the volume is 45 ml.

Via the total number of particles, the volume of the cuvette and the number of particles per ml it is possible to calculate how many liters of particle solution one has to mix into the cuvette to have an optical depth of 5:

$$V_{mix} = V_{\text{cuvette}} \cdot \frac{N_{\text{total}}}{N_\rho} \tag{3.3}$$

which results in

$$V_{mix} = 100\,\mu\text{l} \tag{3.4}$$

of particles to mix into the dye solution. Since the volume change with the added particle is low in comparison to the total volume, it was neglected in the calculation. At first $100\,\mu$l were added to get an optical depth of 5.

[2]The optical depth is the natural logarithm of the ratio of the incident radiant power to the transmitted radiant power through a material [15].

Chapter 4

Result and Discussion

4.1 Spectral Response

The fluorescence spectrum of 1PE and 2PE is shown in figure 4.1. The exposure time was set to 200 ms (1PE) respectively 1500 ms (2PE). Even though the excitation differs, the emission of the fluorescence signal is in theory the same. Therefore the shape of the two spectra should be the same. It is difficult to compare the spectra since the power and the excitation cross section of 1PE and 2PE are different. The peak of the 1PE fluorescene is red shifted in comparison to the peak of 2PE fluorescence. This is a sign of reabsorption due to an overlap of the excitation and emission spectrum of fluorescein. A reason why 1PE is red shifted is that 1PE has a greater excitation cross section. More light gets absorb in the 1PE case than in the 2PE. Consequently, reabsorbtion is stronger in the 1PE peak. The signal of 2PE fluorescence was low and thus experimentally difficult to capture. The peak at 790 nm originates from the light of the Ti:sapphire laser.

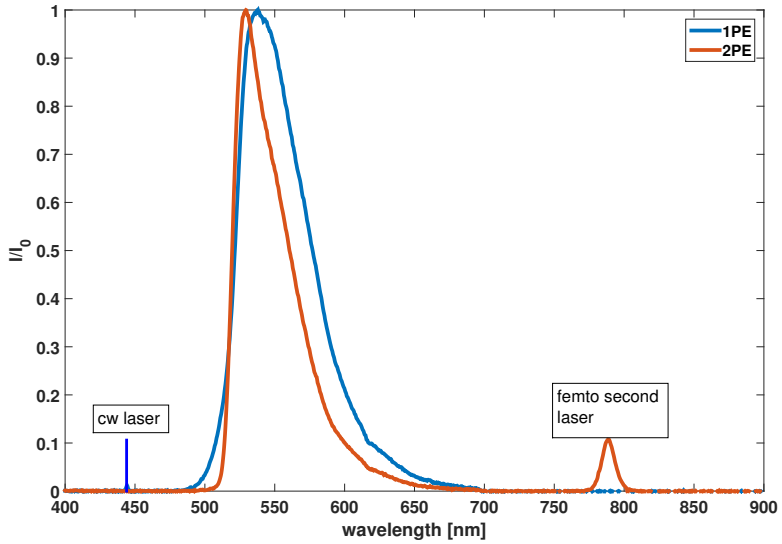

Figure 4.1: The fluorescence spectrum of fluorescein when excited by 447 nm or 790 nm.

4.2 Effects of Dye Concentration and Beam Focusing

Figures 4.2 and 4.3 show the fluorescence image for 1PE and 2PE respectively for different concentration and focal lenses.

The images of 1PE clearly show that at a concentration above 0.0021% the fluorescence signal is located at the entrance and does not penetrate inside the cuvette, while the signal of 2PE increases as a function of to the dye concentration.

Furthermore, the focusing lens does not effect the shape of the emitted fluorescence for 1PE, in contrast to 2PE, where the focusing lens determines the shape of the emitted fluorescence. For a focal length of 75 mm the signal of 2PE fluorescence is emitted locally and has its maximum at the focal point, while the emitted signal remains low along the rest of the beam. At longer focal lengths of the cylindrical lens, the signal at the focal point decreases and the area with high intensity stretches over the cuvette length. With a focusing lens $f = 150\,\text{mm}$ the shape of the signal at the focal point is not clear recognizable anymore as it was in the previous case. There is still an intensity change visible along the beam, but it is significantly less apparent than in the other cases. The fluorescence signal of 2PE represents the diverging shape of the lens.

Short focal length results in a higher signal for 2PE, therefore another measurement of 1PE and 2PE fluorescence was taken with focusing lens f=50 mm, see figure 4.4. The focal length of 50 mm provides the highest peak signal. The fluorescence signal of 2PE is emitted locally at the focal point of the lens, the signal is very low along the rest of the beam.

To conclude, the focal length of the cylindrical length determines the shape of the fluorescence image for 2PE, but does not significantly effect the shape of the 1PE fluorescence image. 1PE fluorescence saturates at the entrance of the cuvette for a concentration above higher than 0.0007%, while 2PE does not. The signal strength increases in respect to dye concentration.

Due to the low signal-to-noise ratio of the 2PE fluorescence images, the lens with the shortest focus (f=50 mm) and therefore the highest signal was used for further experiments.

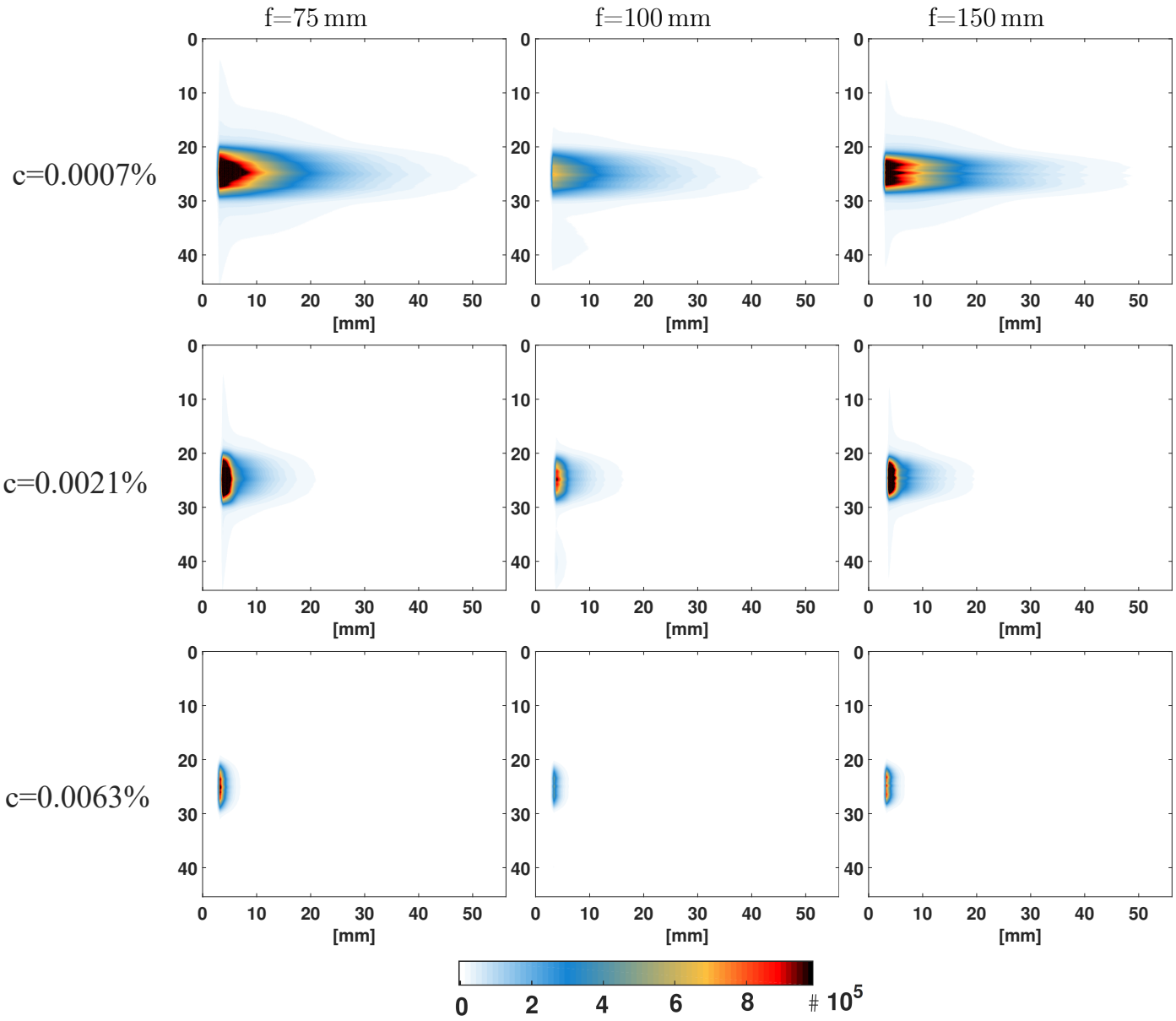

Figure 4.2: The fluorescent image of 1PE with different cylindrical lenses (columns) of focal length 75, 100 or 150 mm and different dye concentrations (indicated on the left side).

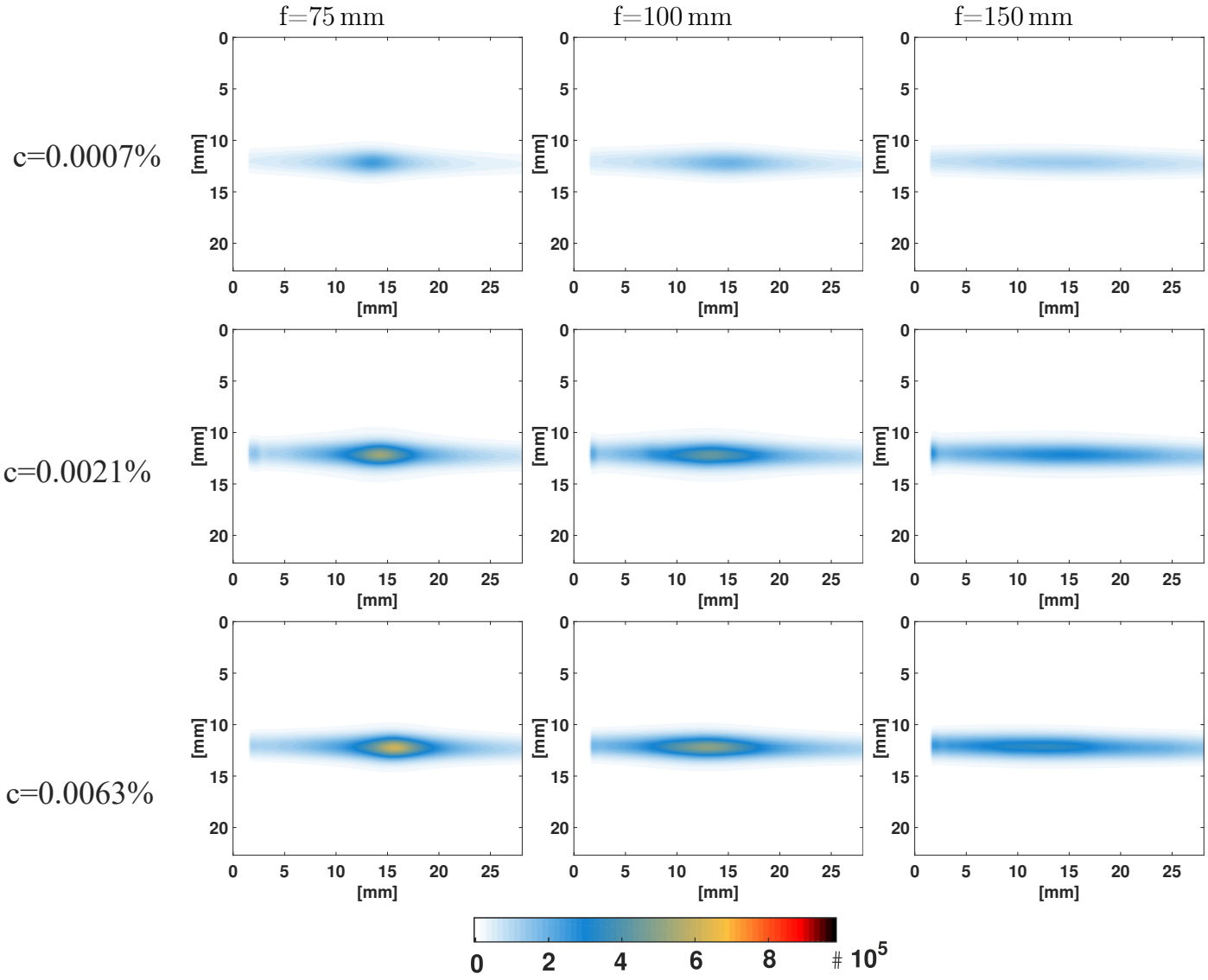

Figure 4.3: The fluorescent image of 2PE with different cylindrical lenses (columns) of focal length 75, 100 or 150 mm and different dye concentrations (indicated on the left side).

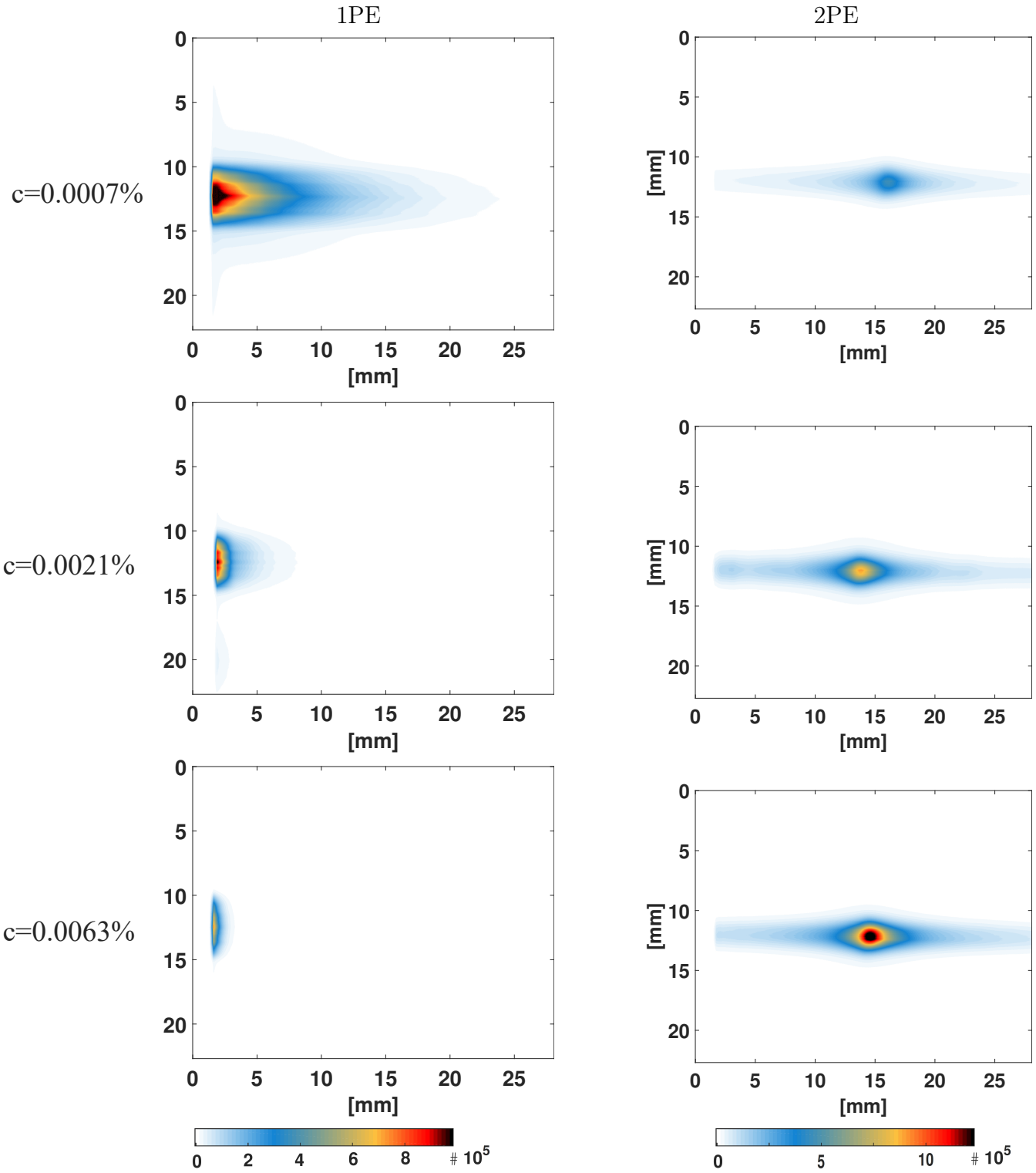

Figure 4.4: The fluorescent image for 1PE and 2PE with the same cylindrical focusing lens, $f = 50\,\text{mm}$ and different dye concentrations (indicated on the left side).

Figure 4.5 shows the normalized intensity vertically integrated over the beam along the cuvette. The plots underline that 1PE independently of the focusing lens peaks at the entrance of the cuvette and decays exponentially. For 2PE fluorescence the signal peaks at the focal point of the focusing lens. When the focusing length is shorter, the peak becomes narrower and vice versa.

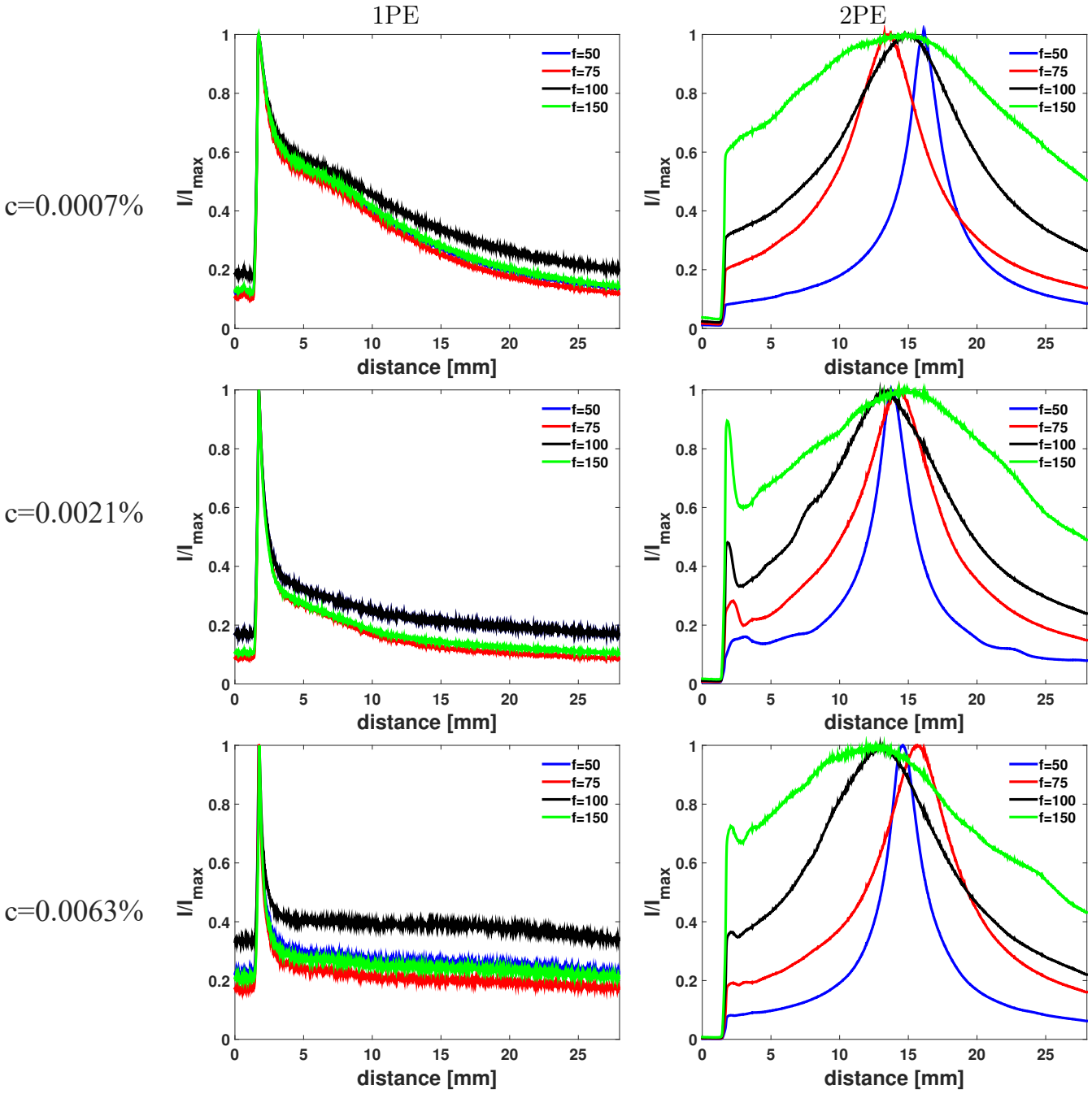

Figure 4.5: The normalized intensity along the cuvette for 1PE and 2PE for different focal lenses at different concentrations (indicated on the left side).

The absolute intensity along the cuvette is plotted in figure 4.6. The shorter the focal length of the focusing lens, for 2PE the higher the signal. For 1PE there is no correlation visible between focal length of the focusing lens and signal strength. The variation of the signal for different focal lengths is probably due to fluctuations of the power of the diode laser.

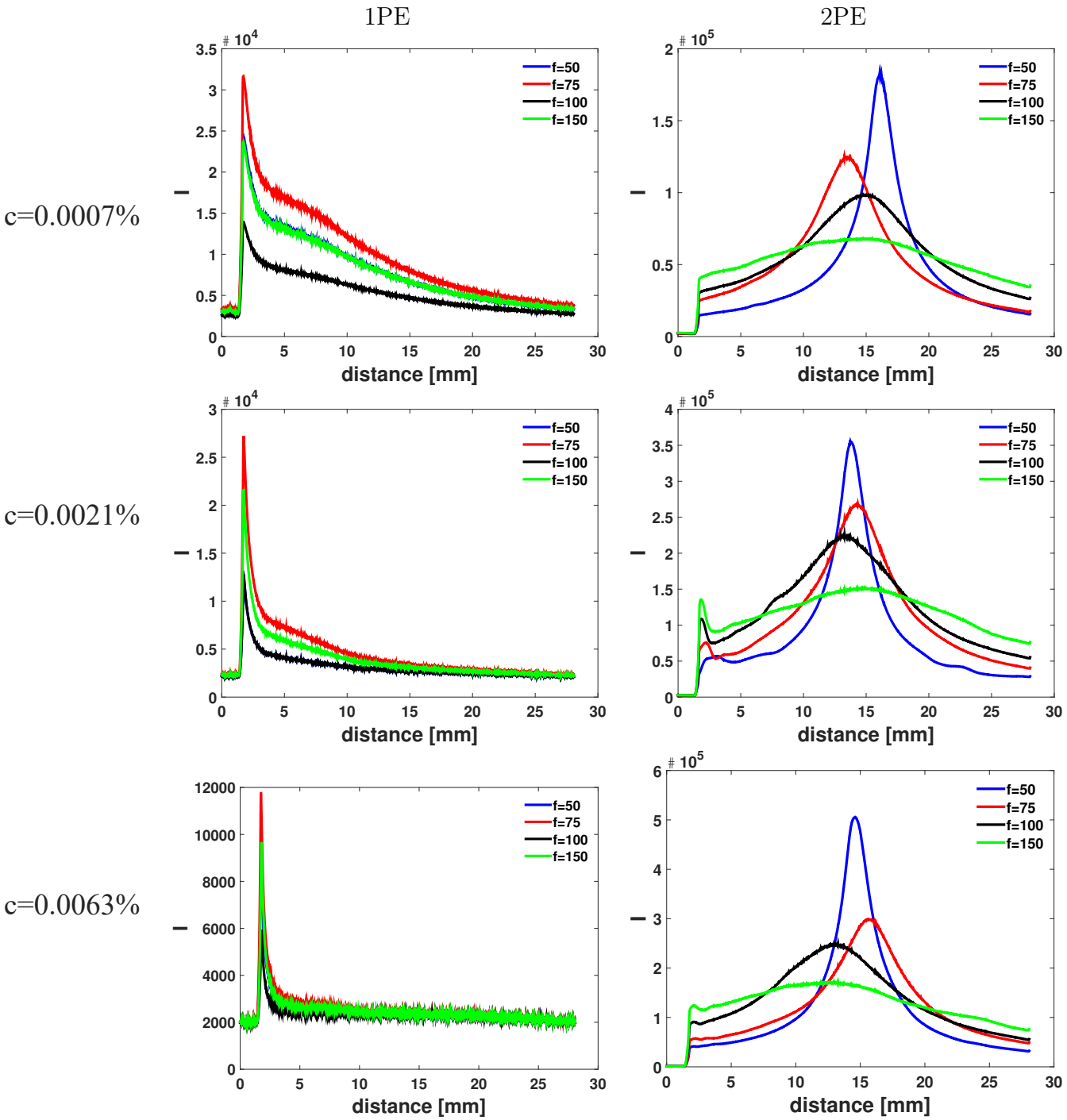

Figure 4.6: The intensity along the cuvette for 1PE and 2PE for different focal lenses at different concentrations (indicated on the left side).

4.3 Imaging in a Controlled Scattering Medium

Beam Profile Analysis

In this experiment, the field of view was smaller than in the previous measurement. Therefore the intensity of the photons was distributed over more pixel, making the signal per pixel decreasing. By mixing the 4.94 μm particles into the solution, the signal decreased, as shown in figure 4.7. Since the signal was low, the exposure time for two-photon excitation had to be increased up to 1 s for 2PE.

The peak in intensity is still at the entrance of the cuvette for 1PE and at the focal point for 2PE. For 2PE the fluorescence signal around the focal point is broaden at higher particle optical depth. Although 2PE is very unlikely to occur outside the focal point, the photon density is high enough around the focal point so that the scattered light can still induce fluorescence. When the distance to cross within the cuvette is increased, the penetration depth of 1PE decreases, as shown in figure 4.7g, 4.7j compared to figure 4.7d.

When the distance to cross within the cuvette is increased from 1 cm (figure 4.7e) to 2 cm (figure 4.7h) the signal at the focal point is reduced by a factor of 2. If the distance is further increased to 3 cm (figure 4.7k), the signal at the focal point is reduced by a factor of 4 compared to 1 cm to cross within the cuvette.

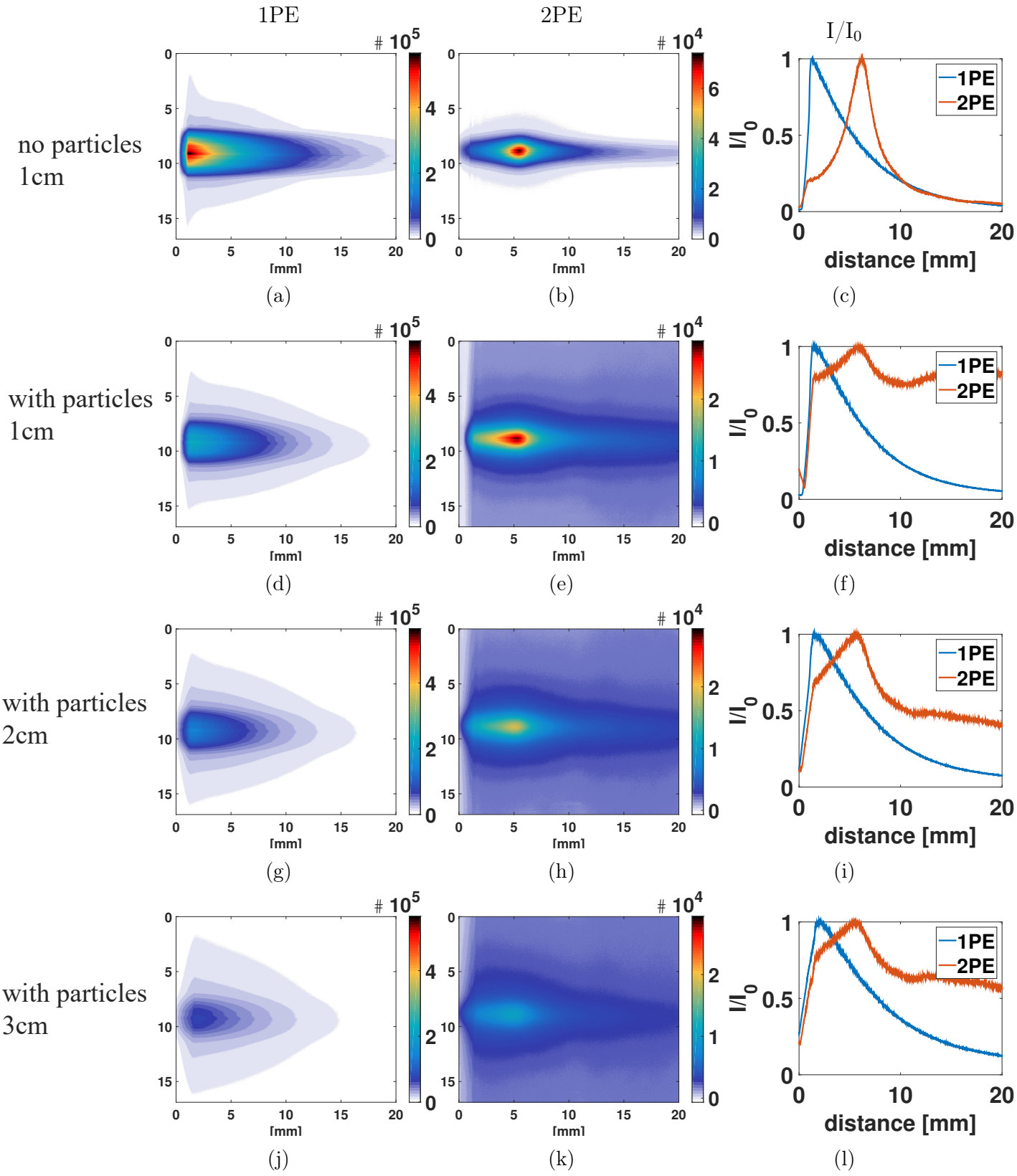

Figure 4.7: Images of 1PE and 2PE fluorescence with and without particles and different distances (1 cm, 2 cm and 3 cm) to cross within the cuvette. The column on the right shows the relative intensity along the cuvette.

Image Contrast Analysis

Figure 4.8 shows the fluorescence signal induced by a spatially modulated light sheet. The signal of 2PE was even without the particles low (200k counts, 600k saturation).

The intensity along a vertical line at the focal point is plotted in the rightmost column. It seems from those intensity profiles that the background of the vertical signal of 2PE without particles (figure4.8b) is lower than the background of 1PE fluorescence (figure 4.8a) by a factor of 8. However, the modulation (peak intensity subtracted by the background) of 1PE without particles is 2.5 times higher than the modulation of 2PE. The modulation of 1PE and 2PE decreases by a factor of 9 and 8 respectively, when particles are added to the aqueous dye solution. When the distance is increased from 1 to 3 cm the signal of 1PE and 2PE is decreased by a factor of 3.2 respectively 3.7, compare figures 4.8d and 4.8e to 4.8g and 4.8h.

The contrast of the images (figure 4.8) is plotted in figure 4.9. The contrast peaks at 6.5 mm 0.4 mm behind the peak in intensity. Without particles the M_f of 2PE is 1.8 times higher at the focal point. At higher OD the signal decreases as well as the contrast. At OD5 and 1 cm to cross in the cuvette M_f of 1PE is 1.5 times higher than for 2PE. The background is high in this configuration in comparison to the other picture at same exposure time and longer distance to cross, which indicates that there was an error in the experimental recording of figure 4.8e.

The high background can be the reason for the strong reduction in image contrast.

The global maximum for particle OD5 and 2 cm to cross is generally higher, for 1PE except for the focal point where the M_f of 2PE exceeds by a factor of 1.1. At the longest distance to cross 1PE performs better than 2PE, expect at the focal point, there the M_f of 2PE is higher. At the focal point at OD5 the intensity has decreased by a factor of 0.7 compared to OD0 due to the present of the particles. Since the process of 2PE depends quadratically on the intensity of the incoming laser, this is a reduction of 0.5 of the fluorescence signal. Due to the low starting signal this reduction has a strong impact on the contrast, as shown in figure 4.8.

From figure 4.8 it is evident that the point to image can be chosen by selecting an appropriate focusing lens. 2PE fluorescence has potential to further increase the contrast, if a more powerful laser or a dye with a higher 2PE cross-section is employed.

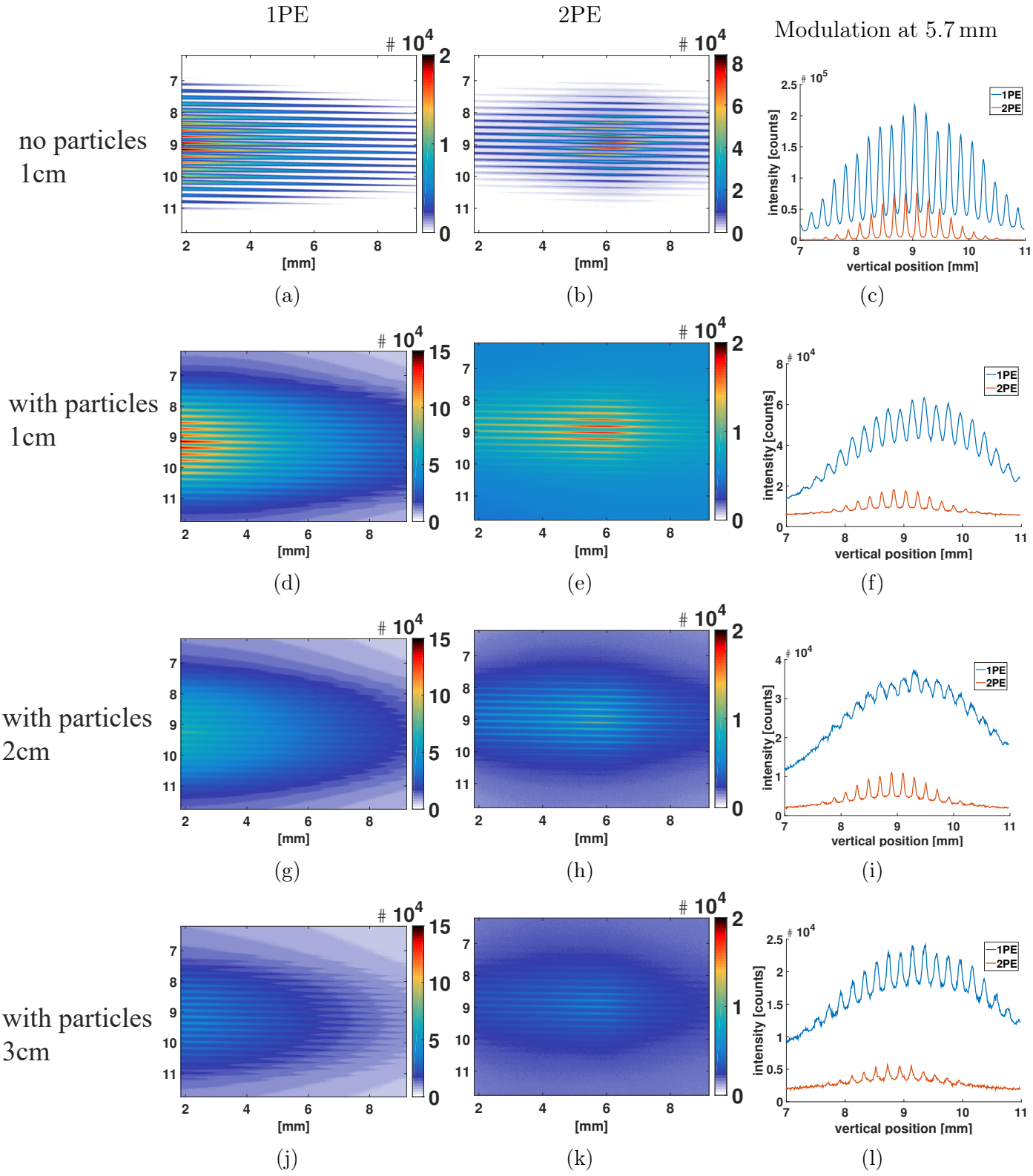

Figure 4.8: Images of 1PE and 2PE fluorescence with and without particles and different distances (1 cm, 2 cm and 3 cm) to cross within the cuvette. The column on the right shows the corresponding modulation at position 5.7 mm of 1PE and 2PE fluorecence.

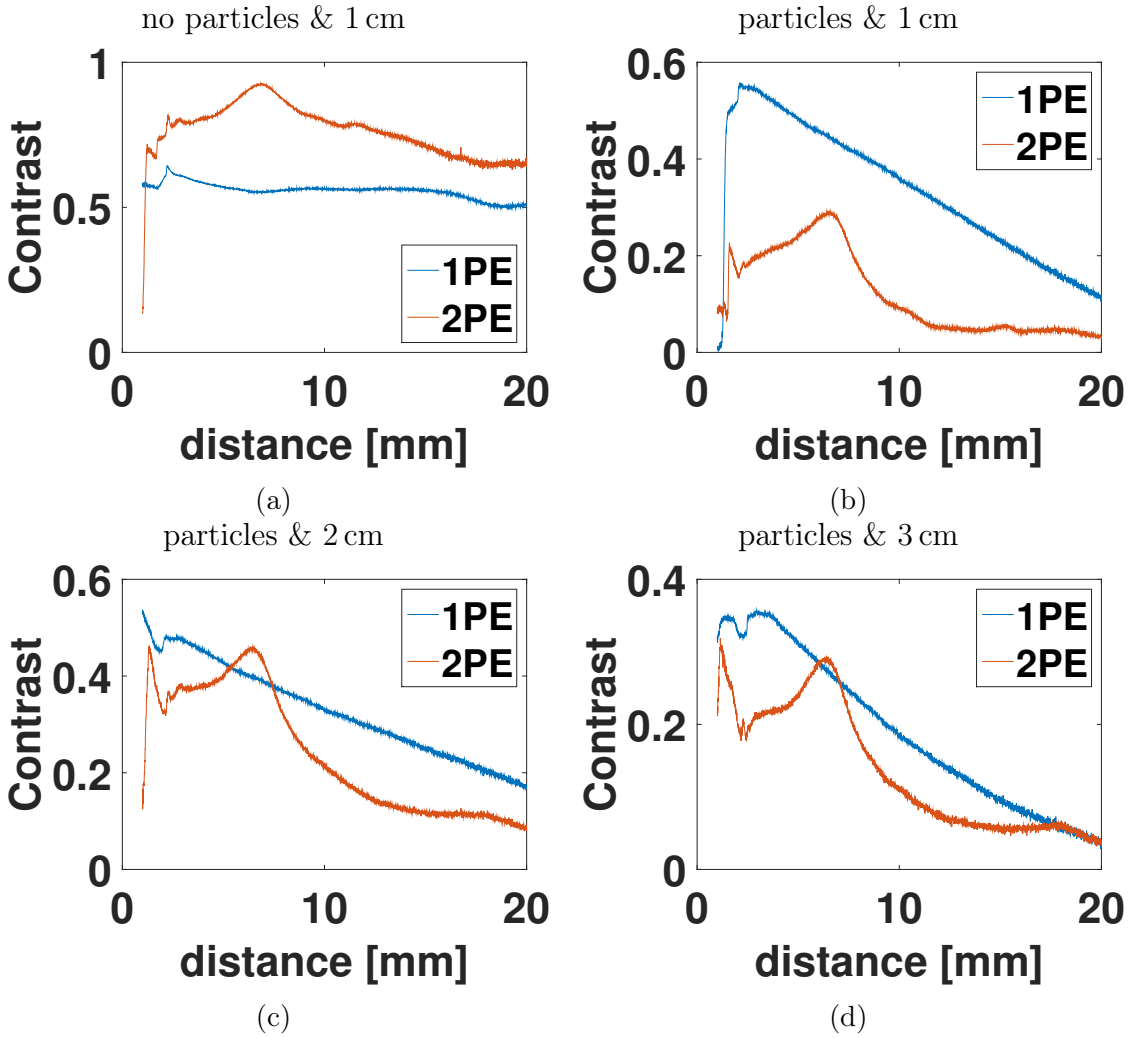

Figure 4.9: The image contrast along the cuvette for 1PE and 2PE with and without particles and different distance to cross within the cuvette.

Chapter 5

Conclusion/Outlook

In this master project several observations have been made; and are listed below:

- First, Fluorescein was proved to be a good candidate for 1PE as well as 2PE fluorescence imaging.
- Moreover, 2PE fluorescence nature showed characteristics that can cope with the planar imaging problems, such as the laser extinction. Since the process depends quadratically on the laser intensity, one can balance the loss of light due to laser extinction by placing a focusing lens with appropriate focal.
- Despite the low SNR, the image contrast from 2PE fluorescence was higher than 1PE fluorescence without any particles in the aqueous dye solution
- When particles, were mixed into the dye solution to increase the optical depth, the contrast of 2PE fluorescence dropped below the contrast of 1PE. A reason for this unwanted behavior was probably be the low starting value in SNR and the high exposure time of 1 s for 2PE.

If one wants to further improve 2PE florescence, a way would be to find a dye with a higher 2PE cross-section. In addition, the dye should have a low 1PE cross-section to avoid reabsoprtion of the 2PE fluorescence signal. Another way to optimize the process would be to use a laser with a higher peak power. Additionally, the repetition rate of the Ti:sapphire laser 80 MHz was too high for single shot imaging.

To conclude, with the limited peak power of 8.75 nJ/pulse and the high repetition rate it was not possible to show the theoretically proposed advantage of 2-photon excitation in a scattering environment. Therefore a laser system with a lower repetition rate for single shot imaging and a higher peak power would be needed to establish the validity of the concept.

Bibliography

[1] Georges A. Wagnieres, Willem M. Star, and Brian C. Wilson. In vivo fluorescence spectroscopy and imaging for oncological applications. Photochemistry and Photobiology, 68(5):603–632, 1998.

[2] Stefan Andersson-Engels, Claes af Klinteberg, K Svanberg, and S Svanberg. In vivo fluorescence imaging for tissue diagnostics. Physics in Medicine and Biology, 42(5):815, 1997.

[3] S. Som. Development and Validation of Spray Models for Investigating Diesel Engine Combustion and Emissions. University of Illinois at Chicago, 2009.

[4] S. G. Demos and R. R. Alfano. Temporal gating in highly scattering media by the degree of optical polarization. Opt. Lett., 21(2):161–163, Jan 1996.

[5] Harsh Purwar, Saïd Idlahcen, Claude Rozé, David Sedarsky, and Jean-Bernard Blaisot. Collinear, two-color optical kerr effect shutter for ultrafast time-resolved imaging. Opt. Express, 22(13):15778–15790, Jun 2014.

[6] E. Berrocal, E. Kristensson, M. Richter, M. Linne, and M. Aldén. Application of structured illumination for multiple scattering suppression in planar laser imaging of dense sprays. Opt. Express, 16(22):17870–17881, Oct 2008.

[7] H. A. Collins M. Pawlicki and H. L. Anderson R. G. Denning. Two-photon absorption and the design of two-photon dyes. Angewandte Chemie International Edition, 48(18):3244–3266, 2009.

[8] C Xu, W Zipfel, J B Shear, R M Williams, and W W Webb. Multiphoton fluorescence excitation: new spectral windows for biological nonlinear microscopy. Proceedings of the National Academy of Sciences, 93(20):10763–10768, 1996.

[9] Semere Ghebru Bairu. Ultrafast Dynamics and Two-Photon Absorption Properties of Chromophores at Interfaces. PhD thesis, 2013.

[10] Manuel E. Zevallos L., S. K. Gayen, M. Alrubaiee, and R. R. Alfano. Time-gated backscattered ballistic light imaging of objects in turbid water. Applied Physics Letters, 86(1), 2005.

[11] M. Linne. Imaging in the optically dense regions of a spray: A review of developing techniques. Progress in Energy and Combustion Science, 39:403–440, 2013.

[12] M. A. A. Neil, R. Juškaitis, and T. Wilson. Method of obtaining optical sectioning by using structured light in a conventional microscope. Opt. Lett., 22(24):1905–1907, Dec 1997.

[13] D. S. Elson, J. Siegel, S. E. D. Webb, S. Leveque-Fort, D. Parsons-Karavassilis, M. J. Cole, P. M. W. French, D. M. Davis, M. J. Lever, R. Juskaitis, M. A. A. Neil, L. O. Sucharov, and T. Wilson. Wide-field fluorescence lifetime imaging with optical sectioning and spectral resolution applied to biological samples. Journal of Modern Optics, 49(5-6):985–995, 2002.

[14] W. Demtröder. Experimentalphysik 2: Elektrizität und Optik. Springer-Lehrbuch. Springer Berlin Heidelberg, 2014.

[15] Terry Renner. Quantities, Units and Symbols in Physical Chemistry. The Royal Society of Chemistry, 2007.